HHS Public Access

Author manuscript

Neuron. Author manuscript; available in PMC 2025 January 03.

Published in final edited form as:

Neuron. 2024 January 03; 112(1): 113–123.e4. doi:10.1016/j.neuron.2023.09.039.

Mast cell-specific receptor mediates alcohol withdrawal-associated headache in male mice

Hyeonwi Son[1], **Yan Zhang**[1], **John Shannonhouse**[1], **Hirotake Ishida**[1], **Ruben Gomez**[1], **Yu Shin Kim**[1,2,3,*]

[1]Department of Oral & Maxillofacial Surgery, School of Dentistry, University of Texas Health Science Center at San Antonio, San Antonio, TX USA

[2]Programs in Integrated Biomedical Sciences, Translational Sciences, Biomedical Engineering, Radiological Sciences, University of Texas Health Science Center at San Antonio, San Antonio, TX USA

[3]Lead contact

SUMMARY

Rehabilitation from alcohol addiction or abuse is hampered by withdrawal symptoms like severe headaches, which often lead to rehabilitation failure. There is no appropriate therapeutic option available for alcohol withdrawal-induced headaches. Here, we show the role of the mast cell-specific receptor MrgprB2 in the development of alcohol withdrawal-induced headache. Withdrawing alcohol from alcohol-acclimated mice induces headache behaviors, including facial allodynia, facial pain expressions, and reduced movement, such symptoms often observed in humans. Those symptoms were absent in MrgprB2-deficient mice during alcohol-withdrawal. We observed *in vivo* spontaneous activation and hypersensitization of trigeminal ganglia neurons in alcohol-withdrawal WT mice, but not in alcohol-withdrawal MrgprB2-deficient mice. Increased mast cell degranulation by alcohol-withdrawal in dura mater was dependent on the presence of MrgprB2. The results indicate that alcohol-withdrawal causes headache via MrgprB2 of mast cells in dura mater, suggesting that MrgprB2 is a potential target for treating alcohol withdrawal-related headache.

eTOC Blurb

*Correspondence: kimy1@uthscsa.edu.

AUTHOR CONTRIBUTIONS

H.S. and Y.S.K contributed to study design. H.S., J.S., and Y.S.K. contributed to data interpretation and manuscript revision. H.S. conceived the project and performed all experiments except as noted and drafted the paper. Z.Y. performed HEK293 cell work. H.S. and J.S. maintained, set up mating, took care of mice, and performed genotyping. H.I. and R.G. assisted with von Frey test work. Y.S.K. supervised all aspects of the project and wrote the paper.

DECLARATION OF INTERESTS

The authors declare no competing interests.

Son et al. show that activation of the mast cell-specific receptor MrgprB2 in the dura mater of male mice causes mast cell degranulation and sensitization of sensory neurons, resulting in headache after alcohol withdrawal.

Keywords

Alcohol withdrawal; Alcohol use disorder; Headache; Primary sensory neuron; CRF; Trigeminal ganglia; Dura mater; GCaMP *in vivo* imaging; Mast cell; MrgprB2; Pain

INTRODUCTION

Alcohol is an addictive substance, and approximately 380 million people suffer from alcohol abuse or dependence (WHO, 2016). Global disasters, such as terrorism, economic adversity, and the COVID-19 respiratory epidemic, are associated with increased alcohol consumption and increased vulnerability to development of risky drinking behaviors[1]. Rehabilitation from alcoholism is of critical importance to managing alcohol dependency in a substantial portion of the population. However, the rehabilitation process is hindered by alcohol withdrawal symptoms, specifically, headache[2–4]. The temporary relief from alcohol withdrawal-induced headache pain derived from resumption of alcohol consumption is an important factor in the failure to break the addiction cycle[5,6], seriously affecting quality of life and aggravating alcohol dependence. Despite a major unmet medical need for treating alcohol withdrawal-induced headache, there is no appropriate therapeutic option available. To develop better therapeutics, it will be necessary to obtain a clearer understanding of alcohol withdrawal-induced headache pain mechanisms.

Headache is initiated from the activation of trigeminal ganglia (TG) neuronal afferents and vasodilation in dura mater. Processes that cause local inflammation of dura mater sensitize peripheral afferents of TG neurons[7–9], and their activation by mechanical and chemical stimuli contribute to the progression of general headaches[7,10]. Mast cell degranulation in dura mater has been implicated in local inflammation and nociceptive afferent activation of TG neurons and vasodilation[11,12], suggesting that activated mast cells in dura mater may mediate headache. Mast cells are located proximal to peripheral nerve endings and peripheral blood vessels in dura mater, where they can be activated by various secretagogues to release proinflammatory cytokines[13,14]. Mas-related G-protein-coupled receptor B2 (MrgprB2), which is selectively expressed on connective tissue mast cells, is activated by basic secretagogues[15] and mediates neurogenic inflammation pain[16–18]. Chronic alcohol consumption induces increased mast cell numbers and degranulation in peripheral tissues, contributing to inflammation[19–21]. In view of these observations, we tested whether mast cell-specific MrgprB2 contributes to alcohol withdrawal-induced headache.

RESULTS

Mast Cell-Specific Receptor, MrgprB2 Mediates Alcohol Withdrawal-Induced Headache Behaviors

In a two-bottle (10% ethanol vs. water) voluntary choice paradigm, mice exhibited a preference for ethanol (Figure S1A). Neither food intake (Figure S1D) nor body weight (Figure S1C) were affected. Ethanol intake increased gradually over the three-week study (Figure S1B), indicative of developing ethanol dependence. MrgprB2 deficiency did not significantly inhibit development of ethanol preference/intake over 3 weeks (Figure S1A and B). In WT mice, withdrawal from voluntary ethanol access after 3 or 8 weeks induced mechanical hypersensitivity in the periorbital area, which was maintained for up to 4 days (Figure 1A and S3O). Moreover, the grimace pain score was significantly increased 24 hours after alcohol withdrawal (Figure 1B and S1E). Reduced exploratory behaviors in the open field test after alcohol withdrawal in mice (Figure 1C and S1F) correlated with avoidance of physical activity described in migraineurs[22]. However, these headache behaviors induced by alcohol withdrawal were absent in MrgprB2-deficient (MrgprB2 KO) mice (Figure 1A–C). Thus, these findings show that withdrawal from ethanol in WT mice but not in MrgprB2 KO mice resulted in headache behaviors, suggesting that mast cell-specific MrgprB2 mediates alcohol withdrawal-induced headache.

Mast Cell Activation via MrgprB2 in Dura Mater Contributes to Alcohol Withdrawal-Induced Sensitization of TG Neurons

To assess the effects of ethanol withdrawal on TG neurons after 3 weeks of alcohol access, we monitored the activity of TG neurons in live animals using *in vivo* intact TG Pirt-GCaMP3 Ca^{2+} imaging (Figure S6). The total number (>134±6.02) of spontaneously activated TG neurons was dramatically increased in WT alcohol-withdrawal mice compared to water-fed controls (Figure 1D–F). The spontaneously activated neurons included neurons exhibiting Ca^{2+} oscillations and neurons with steady-state high Ca^{2+}, both of which were significantly increased in WT alcohol-withdrawal mice (Figure 1D–F). The group of small-diameter (<20 μm) and medium-diameter (20–25 μm) neurons from alcohol-withdrawal mice showed more spontaneously activated neurons than water-fed controls (Figure 1G and S1G). The numbers of spontaneously activated TG neurons were significantly decreased in alcohol withdrawal of MrgprB2-deficient mice (Figure 1D–G). Ethanol consumption is known to modulate mast cell activities, including increasing degranulation[19–21]. Indeed, numbers of degranulated mast cells (Figure 1H) and total numbers of mast cells (Figure S2A) were increased in dura mater of ethanol-drinking mice, and these increases were abolished in MrgprB2-deficient mice (Figure 1H and S2A). These data indicate that MrgprB2 is required for mast cell degranulation evoked by alcohol withdrawal, suggesting that mast cell activation via MrgprB2 results in development of alcohol withdrawal-induced headache and pain behaviors.

CRF, MrgprB2 Activator, in Dura Mater Induces Headache Behaviors

Our findings indicate that degranulation of mast cells via MrgprB2 sensitizes TG neurons to evoke alcohol withdrawal-induced periorbital mechanical hypersensitivity and pain behaviors, but it remains unclear how alcohol withdrawal mediates activation of MrgprB2

leading to degranulation of mast cells. We sought to identify a putative activator of MrgprB2 after alcohol withdrawal. Alcohol consumption and withdrawal is known to activate the hypothalamic-pituitary-adrenal (HPA) axis[23–27]. We postulated that Corticotropin-releasing factor (CRF), a hormone active in regulating HPA axis function, might be involved in MrgprB2 activation and subsequent development of alcohol withdrawal-induced headache[28,29]. We found significantly increased CRF levels in plasma (Figure 2B) and increased expression (Figure S2B and S2C) in the dura mater of alcohol-withdrawal mice compared to water-fed controls. It is likely that the increased CRF level in dura mater was a consequence of the high CRF level in plasma. Since CRF, a secretagogue of mast cells, induces mast cell degranulation[30], we hypothesized that CRF-induced activation of mast cells mediates alcohol withdrawal-induced headache behaviors. We found that CRF increased degranulation in mouse mast cells isolated from the peritoneal cavity, and this increase was absent in mast cells isolated from MrgprB2-deficient mice (Figure 2C). We next asked whether local increases of CRF in dura mater induce headache-like and pain behaviors. To test this, we directly injected CRF into dura mater. CRF injection significantly induced periorbital mechanical hypersensitivity from 1 to 24 hours post-injection, which returned to baseline within 72 hours (Figure 2D). This was similar to the effect of IL-6, which is a well-known periorbital mechanical hypersensitivity inducer[31,32]. However, MrgprB2-deficient mice did not show periorbital hypersensitivity following dural CRF injection (Figure 2D). Recent studies reported that MrgprB2 responds to various positively charged protein-secretagogues[15,33], which led us to test whether CRF directly activates MrgprB2. We confirmed that CRF induced Ca^{2+} transients in HEK293 cells expressing MrgprB2 or the human ortholog MrgprX2 (Figure 2E and F). We also applied CRF onto isolated mouse mast cells and cultured LAD2 human mast cells *in vitro* and found that the CRF application also evoked Ca^{2+} transients in isolated mouse mast cells and LAD2 human mast cells (Figure 2G and H). To rule out the possibility that CRF indirectly activated MrgprB2 in mast cells by engaging CRF-induced Ca^{2+} transients via CRF receptors[34], we added astressin, a CRF 1/2 receptor inhibitor, before CRF application. Astressin treatment did not block CRF-induced Ca^{2+} transients in isolated mouse mast cells or LAD2 human mast cells but did increase Ca^{2+} transients (Figure S2F and S2G). Consistent with this result, astressin injection into dura mater enhanced the effect of CRF on periorbital mechanical hypersensitivity (Figure S2E). We confirmed that the CRF-induced Ca^{2+} transients were absent in mouse mast cells isolated from MrgprB2-deficient mice (Figure S5A), indicating that CRF activates mast cells via MrgprB2. In addition, using *in vivo* intact TG Pirt-GCaMP3 Ca^{2+} imaging, we found a significant increase in the number of activated neurons following dural CRF injection (Figure 2I). In *in vivo* dura mater imaging, direct CRF application onto dura mater induced vasodilation (Figure 2J), a primary event occurring during migraine and headaches[7,35]. These results indicate that CRF, which is likely released from dural blood vessels, induces mast cell degranulation via MrgprB2 activation, and regulates development of alcohol withdrawal-induced headache and pain behaviors by sensitization of TG nerve in dura mater.

MrgprB2 Contributes to Alcohol Withdrawal-Induced Sensitization of TG nerves

From studies identifying the pathophysiology of migraine headache, it is known that cutaneous allodynia is observed in response to non-noxious stimulation of periorbital

and forehead skin areas during headache[36]. To confirm sensitization of TG nerve with various stimuli, including mechanical, thermal, and chemical stimuli, we applied von Frey filament (mechanical), hot water (thermal), or capsaicin (chemical) to each orofacial region innervated by ophthalmic (V1), maxillary (V2), or mandibular (V3) branches of TG nerves during *in vivo* intact TG Pirt-GCaMP3 Ca^{2+} imaging. Application of 0.4 g to the V1 region, but not to V2 or V3 regions, increased activation of TG neurons in alcohol-withdrawal mice (Figure 3B and S3A, H). This signal was due to increased activation of small-diameter to medium-diameter neurons (Figure 3B). Mild hot water (40°C) or acetone (cold stimulus) applications also revealed greater numbers of activated TG neurons in V1 region but not in V2 or V3 regions (Figure 3C and S3C, E, J, L). The number of small to medium-diameter neurons activated in V1 region was increased in response to mild hot water (40°C) in alcohol-withdrawal mice (Figure 3C). Capsaicin injection into the V1 region but not in V2 or V3 regions of alcohol-withdrawal mice resulted in an increase in activated TG neurons (Figure 3D and S3G, N). The sensitization of TG neurons in V1 region was observed in alcohol-withdrawal mice up to 8 weeks following withdrawal from voluntary ethanol consumption (Figure S3P–S3S). Consistent with the results of headache and pain behaviors, MrgprB2-deficient mice after alcohol withdrawal did not exhibit an increase in activated TG neurons relative to control groups in response to all stimuli in all three branches (Figure 3B–D). Collectively, these results suggest that alcohol-withdrawal mice exhibit sensitization of TG nerve by mechanical, thermal, and chemical stimuli and suggest that the mast cell-specific receptor MrgprB2 contributes to alcohol withdrawal-induced sensitization of TG nerves responsible for inducing headache and pain behaviors.

Alcohol Withdrawal Induces Hypersensitivity of Hindpaw and Sensitization of DRG Neurons

Consistent with previous studies[37–39], mice conditioned by voluntary ethanol consumption for 3 to 8 weeks, exhibited hypersensitivity in hindpaw following alcohol withdrawal (Figure 4A and S4A), which lasted for 5 days after withdrawal. Importantly, MrgprB2 deficiency did not prevent alcohol withdrawal-induced hypersensitivity in hindpaw (Figure 4A). To examine whether sensitization of dorsal root ganglia (DRG) neurons occurs in mice following alcohol withdrawal, we also monitored neuronal activation by *in vivo* intact DRG Pirt-GCaMP3 Ca^{2+} imaging. Mild (100 g) or noxious (300 g) press to the hindpaw of alcohol-withdrawal mice significantly increased the number of activated DRG neurons compared to water-fed controls (Figure 4C–H and S4B–C). In response to these stimuli, small- and medium-diameter neurons were significantly more activated in DRG of alcohol-withdrawal mice than water-fed controls (Figure 4E and 4H). We also found an increase in activated neurons in the DRG of alcohol-withdrawal mice in response to noxious heat (50°C) (Figure 4I–K and S4D). The numbers of small- and medium-diameter neurons activated by noxious heat were significantly higher in alcohol-withdrawal mice than in water-fed controls (Figure 4K and S4D).

Alcohol Withdrawal-Induced Headache Behavior is Mediated by TNF-α and TRPV1.

To identify specific molecular signaling mechanisms that drive hypersensitivity in different anatomical locations as a result of alcohol withdrawal, we investigated whether inhibition of tumor necrosis factor-α (TNF-α) receptor, which was increased by alcohol consumption[40],

would block alcohol withdrawal-induced mechanical allodynia. TNF-α levels in dura mater were increased by alcohol withdrawal, but not in MrgprB2-deficient mice (Figure S5B). Furthermore, we found that alcohol withdrawal-induced mechanical allodynia in hindpaw or in the head was blocked by R-7050, a TNF-α receptor inhibitor (i.p. injection for 11 consecutive days) (Figure 4L and 4M). A recent study suggested that chronic alcohol consumption induces nociceptor sensitization in hindpaw through an increase in reactive oxygen species (ROS)[38], which led us to ask whether ROS production is a consequence of TNF-α release, and if ROS are involved in both hindpaw and head mechanical allodynia. We found that mechanical allodynia in hindpaw of alcohol-withdrawal mice was reversed by PBN, a ROS scavenger, whereas mechanical allodynia in the head was not reversed (Figure 4N and 4O). We also confirmed that the mechanical allodynia in the head caused by alcohol withdrawal was reversed by SB366791, a TRPV1 inhibitor (Figure 4N and 4O). Activated mast cells can release TNF-α, which is a well-known potentiator of TRPV1 ion channel[41], suggesting that in alcohol-withdrawal mice TRPV1 activation is a component of a downstream signaling cascade of mast cell activation via MrgprB2.

DISCUSSION

Clinical observations have indicated that alcohol consumption causes headaches[42–45], although the pathophysiological mechanism remains unknown. Here, we show that withdrawal from alcohol causes headache and pain behaviors, which are associated with sensitization of TG neurons. We also show that CRF directly activates MrgprB2, which mediates alcohol withdrawal-induced behavioral and cellular changes (Figure 4P). Moreover, we identified different signaling mechanisms of alcohol withdrawal-induced hypersensitivity in the head compared with hypersensitivity in hindpaw. These results identify a mechanism of alcohol withdrawal-induced headache and point to a therapeutic target for treating alcohol withdrawal-induced headache and addictive behaviors.

Mast cells in dura mater participate in inflammation and subsequent sensitization of peripheral afferents, events which are thought to be components of a cascade leading to development of migraine headache[12,46]. We here show that CRF activates mast cells via MrgprB2, which causes headache behaviors and TG nerve sensitization. These results indicate that CRF mediates alcohol withdrawal-induced physiological changes and mast cell degranulation which produce headache. Mast cells express CRF1/2 receptors[34,47]. Unlike MrgprB2, CRF receptors act as modulators of mast cell activity. It has been reported that activation of CRF1 receptor enhances calcium transients and calcium signals, and CRF2 receptor suppresses these activities in mast cells[34]. Thus, CRF1 receptor alone is not sufficient to degranulate mast cells[47]. Here, we confirmed that the inhibition of CRF1/2 receptors do not block CRF-induced mast cell activation, and we show that MrgprB2 is required for CRF-induced mast cell Ca^{2+} activation and degranulation, indicating that MrgprB2 is a major receptor mediating CRF-induced mast cell activation. Because expression of CRF receptors changes under various conditions[34], further study is needed to fully elucidate the modulatory role of mast cell CRF receptors following alcohol withdrawal in mice.

CRF induces the release of TNF-α from human mast cells[48,49]. Here, we observed increased CRF and TNF-α levels after alcohol withdrawal and showed that R-7050, an inhibitor of TNF-α receptor, attenuated alcohol withdrawal-induced headache behavior. These findings indicate that CRF/MrgprB2-induced TNF-α release mediates alcohol-induced headache behavior. Since activation of TNF-α receptor leads to sensitization of TRPV1[41] and we found that an inhibitor of TRPV1, SB366791, attenuates alcohol withdrawal-induced headache behavior, we conclude that TNF-α release from mast cells by CRF can mediate sensitization of sensory neurons induced by alcohol withdrawal. However, we did not completely rule out the possibility that other effectors may be involved in CRF/MrgprB2-induced mast cell activation. Nevertheless, the finding that MrgprB2-deficient mice had no elevation of TNF-α and no headache behaviors after alcohol withdrawal emphasizes that MrgprB2 is a key factor in the development of alcohol withdrawal-induced headache behavior.

Pain produced by bidirectional communication between the immune and nervous systems causes animals to maintain homeostasis and to respond to environmental challenges. Mast cells play an important role in this bidirectional communication by releasing bioactive molecules which impact sensory neurons[50]. MrgprB2 and MrgprX2 give mast cells the ability to respond to a large variety of physiological peptides, including substance P, pituitary adenylate cyclase-activating polypeptide (PACAP), somatostatin, and cortistatin-14[15,51]. It has been confirmed that MrgprB2 mediates the regulation of pain sensation in response to substance P in tissue injury[16]. We found that MrgprB2 activated by CRF in mast cells causes alcohol withdrawal-induced headache behaviors, suggesting that mast cell MrgprB2 mediates interactions between abnormal physiological changes and pain system via inducing release of inflammatory factors, and that the headache behaviors observed in this study are a consequence of alcohol withdrawal-induced physiological changes. Given that MrgprB2 deficiency does not influence escalated alcohol consumption, it implies that the escalating alcohol consumption is not determined by sensory representation from dura mater in the absence of alcohol withdrawal-induced physiological changes. Alcohol withdrawal-induced physiological changes and pain are also observed in users of other addictive substances, including heroin and other opioids[52]. Thus, MrgprB2-induced mast cell activation might be a significant signaling pathway in the development of headache induced by addictive substances.

Pain and alcohol dependence have a close relationship. The acute pain-inhibitory effects of alcohol consumption and the acute pain-inducing effects of alcohol withdrawal serve to motivate alcohol consumption, which leads to alcohol dependence[2,4]. Indeed, patients receiving treatment for alcohol use disorder exhibit more significant pain responses during the early stages of alcohol abstinence. In adults with chronic pain, their pain intensity correlates with increased alcohol consumption[4]. Therefore, pain relief, especially from headache, could be a means to lower alcohol dependence[5].

Alcohol abuse or addiction is a significant public health problem, especially so during the COVID-19 pandemic, because the pandemic is leading people to consume more alcohol, increasing their vulnerability to the development of alcohol addictive behaviors[1]. Moreover, pain, including headache, from alcohol withdrawal disrupt rehabilitation from alcohol

dependence[4,5]. Here, we show that blockade of mast cell-specific MrgprB2 attenuates alcohol withdrawal-induced headache behaviors. These results identify MrgprB2 as a possible new therapeutic target for treating alcohol withdrawal-induced headache and alcohol dependence.

STAR METHODS

RESOURCE AVAILABILITY

Lead Contact—Further information and requests for resources and reagents should be directed to and will be fulfilled by the lead contact, Yu Shin Kim (kimy1@uthscsa.edu).

Materials Availability—This study did not generate new unique reagents.

Data and Code Availability

- Raw data used in this study are available upon request.
- This paper does not report original code.
- Any additional information required to reanalyze the data reported in this paper is available from the lead contact upon request.

EXPERIMENTAL MODEL AND STUDY PARTICIPANT DETAILS

Animals—The C57BL/6 mice used in experiments were obtained from The Jackson Laboratory; Pirt-GCaMP3 mice were generated and used as described previously[53,54]. MrgprB2-deficient (KO) mice on a C57BL/6 background were purchased from The Centre for Phenogenomics (Ontario, Canada). All mice spent at least one week in group housing (4–5 mice per cage, 23°C, regular light/dark cycle), and then were split into single housing one week before the experiment. In this study only male mice used for experiments were 8–16 weeks old. Female mice are reported to consume more alcohol than male mice. We have verified this finding. However, to date, we have not confirmed other differences between males and females. All experiments were performed in accordance with a protocol approved by the University of Texas Health at San Antonio (UTHSA) Animal Care and Use Committee (IACUC).

Cell lines—HEK293 cell line, derived from human embryonic kidney cells, was used for our experiments. These cells were maintained in DMEM supplemented with 10% FBS and 1% penicillin-streptomycin at 37°C in a 5% CO_2 humidified atmosphere. LAD2 human mast cells (Laboratory of Allergic Diseases 2), provided by Professor Dr. Xinzhong Dong from Johns Hopkins University (MD, USA), were cultured in StemPro-34 SFM medium (Life Technologies, Carlsbad, CA, USA) supplemented with 2 mM L-glutamine, 100 U/ml penicillin, 50 mg/ml streptomycin, and 100 ng/ml recombinant human stem cell factor (Peprotech, Cranbury, NJ, USA) and were maintained at 37°C, 5% CO_2. Cell culture medium was hemi-depleted every week and replaced with fresh medium.

Mouse mast cell culture—Peritoneal mast cells were isolated from adult male and female mice as previously described[15]. Briefly, 2 × 5 mL of ice-cold mast cell dissociation

medium (MCDM; HBSS with 3% FBS and 10 mM HEPES, pH7.2) was injected into the peritoneal cavity, and the abdomen was massaged for 60s; peritoneal fluid was collected and centrifuged at 200 rcf for 5 min at room temperature. The pellets were resuspended in 2 mL MCDM, layered over 4 mL of an isotonic 70% Percoll solution (MilliporeSigma, St Louis, MO, USA), and centrifuged at 500 rcf for 20 min at 4°C. Purity of isolated mast cells was >95%, as determined from avidin staining. The mast cells were resuspended in DMEM with 10% FBS, 100 U/mL penicillin, 50 mg/mL streptomycin, and 25 ng/mL recombinant mouse stem cell factor (mSCF; Peprotech, Cranbury, NJ, USA) and plated onto glass coverslips coated with 30 mg/mL fibronectin (MilliporeSigma, St Louis, MO, USA).

Alcohol withdrawal model—The voluntary two-bottle choice ethanol drinking paradigm was used for ethanol self-administration[37]. Mice received ad libitum 24 hour access for 3 or 8 weeks to two bottles: one bottle containing water and another bottle containing ethanol. The location of the bottles on the cage was exchanged every other day. The alcohol bottle contained 3% ethanol (days 1–2), 6% ethanol (days 3–4), and 10% ethanol thereafter.

METHOD DETAILS

Peptides and drugs—CRF peptide was purchased from Phoenix Pharmaceuticals (Burlingame, CA, USA). R-7050, PBN, SB366791, and astressin were purchase from Tocris Bioscience/Bio-Techne Corporation (Minneapolis, MN, USA). IL-6 was sourced from R&D Systems (Minneapolis, MN, USA), while PBN was acquired from Cayman Chemical (Ann Arbor, MI, USA). CRF (10 ng), IL-6 (0.1 ng), and astressin (4 ng) were prepared in synthetic interstitial fluid[32] and administered to dura. R-7050 (12 mg/kg), PBN (100 mg/kg), and SB366791 (1 mg/kg) were prepared in 5% DMSO, 5% Tween-80 in 0.9% NaCl and intraperitoneally administered.

Behavior tests (mechanical, grimace, open field)—Hindpaw or facial mechanical von Frey test was performed according to previously published methods[32,37]. Mice were familiarized and habituated to the experimenter's smell, hand touch, and eye contact for at least for 3 days, and then were acclimated in a plexiglass chamber with 4 oz paper cups for 2 hours per day for 3 days. After acclimation, mice were subjected to daily baseline testing of cutaneous facial (periorbital region) or hindpaw sensitivity touched by von Frey filament for approximately 5 days. Withdrawal threshold of the facial von Frey test was determined using the Dixon "up-and-down" method[55]. Baseline threshold was approximately 0.5 to 0.7 g. **Grimace pain behavior** was recorded in five characterized facial areas (orbital, nose, cheek, ears, and whiskers) on a scale of 0 to 2 (0 = not present, 1 = somewhat present, 2 = clearly present) as previously published[56]. **The open field test** was performed in a new cage for 5 min. The mouse's movements were recorded using a video camera, and the movement was analyzed using ImageJ (NIH) with animal tracker (plugin)[57]. All investigators were blinded to experimental conditions.

DRG and TG exposure surgery for *in vivo* intact DRG and TG Pirt-GCaMP3 Ca^{2+} imaging—DRG exposure surgery was performed as previously described[53]. Mice were anesthetized by i.p. injection of Ketamine/Xylazine (approximately 80/10 mg/kg) (MilliporeSigma, St Louis, MO, USA), their backs were shaved and ophthalmic ointment

(Lacri-lube; Allergen Pharmaceuticals) was applied to the eyes. The surface aspect of the L5 DRG transverse process was removed to expose underlying DRG. Bleeding from the bone was stopped using styptic cotton. **For TG exposure surgery**, we first surgically exposed the right-side dorsolateral skull by removing skin and muscle. The dorsolateral skull (parietal bone between right eye and ear) was removed using a dental drill (Buffalo Dental Manufacturing, Syosset, NY, USA) to make a cranial window hole (~10×10 mm). The TG was then exposed where it is located under the brain by aspirating overlying cortical tissue through the cranial window in the dorsolateral skull. The animal was then laid on its abdomen on the stage under a Zeiss LSM 800 confocal microscope (Carl Zeiss). The animal was restrained using a mouse tooth holder to minimize movements from breathing and heartbeats. During the surgery, the body temperature of the mouse was maintained on a heating pad at 37°C ± 0.5°C as monitored by rectal probe.

In vivo Pirt-GCaMP3 Ca^{2+} imaging in DRG and TG—*In vivo* Pirt-GCaMP3 Ca^{2+} imaging in live mice was performed for 2–5 hours immediately after exposure surgery as previously described[53,54]. After the exposure surgery, mice were laid abdomen-down on a custom-designed platform under the microscope objective. For ***in vivo* intact DRG Pirt-GCaMP3 Ca^{2+} imaging**, the spinal column was stabilized using two clamps on vertebra bone above and below the DRG being imaged. Live images were acquired at ten frames per cycle in frame-scan mode per ~4.5 to 8.79 s/frame, ranging from 0 to 900 μm, using a 10 × 0.4 NA dry objective at 512 × 512 pixel or higher resolution with solid diode lasers tuned at 488 nm absorption and emission at 500–550 nm. An average of 1,825±71 neurons per DRG (~10–15% of total DRG neurons) was imaged. For ***in vivo* intact TG Pirt-GCaMP3 Ca^{2+} imaging**, the animal's head was fixed using a custom-designed head holder. During the imaging session, body temperature was maintained at 37°C ± 0.5°C on a heating pad and monitored by rectal probe. Anesthesia was maintained with 1–2% isoflurane using a gas vaporizer, and pure oxygen was delivered through a tooth holder. Live images were acquired at ten frames per cycle in frame-scan mode per ~4.5 to 8.79 s/frame, ranging from 0 to 900 μm, using a 5 × 0.25 NA dry objective at 512 × 512 pixel or higher resolution with solid diode lasers tuned at 488 nm absorption and emission at 500–550 nm. An average of 2,867±87 neurons per TG (~10% of total TG neurons[58,59]) was imaged and small regions of TG neurons were imaged at higher speed >40Hz. von Frey filaments (0.4 g and 2.0 g) were applied to the face or hindpaw of exposed TG branches or DRG side. A rodent pincher (Bioseb, U.S.A.) was used to apply 100 g and 300 g press to the whole palm of the hindpaw. Water at 40°C, 50°C, or 60°C or acetone was applied by pipette to the hindpaw or the different TG branches. Capsaicin (500 mM, 10 μl) or KCl (500 mM, 10 μl) was cutaneously injected into the different TG branches using a 0.5-ml insulin syringe with a 28-gauge needle.

***In vivo* Pirt-GCaMP3 Ca^{2+} imaging data analysis—**For imaging data analysis, raw image stacks were collected, deconvoluted, and imported into ImageJ (NIH). Optical planes from sequential time points were re-aligned, and motion was corrected using the stackreg rigid-body cross-correlation-based image alignment plugin. Ca^{2+} signal amplitudes were expressed as F_t/F_0 as a function of time. F_0 was defined as the average fluorescence intensity during the first two to six frames of each imaging experiment. All responding cells were

verified by visual examination of the raw imaging data. Spontaneous activity from primary sensory neurons has two distinct events, Ca^{2+} oscillating neurons and steady-state high Ca^{2+} neurons without any stimuli. Ca^{2+} oscillating neurons are defined as Ca^{2+} intensity level changes or fluctuations over time. Steady-state high Ca^{2+} neurons are defined as maintaining nonfluctuating Ca^{2+} intensity levels significantly above baseline.

Mouse dural injection—Mouse dura injection was performed as previously described[31]. Mice were anesthetized under isoflurane briefly, and drugs or compounds were injected in a volume of 5 μl via a modified internal cannula (P1 Technologies, Roanoke, VA, USA). The length of the injection needle was adjusted between 0.5 and 0.65 mm.

***In vivo* blood vessel imaging in dura mater—**Mice were anesthetized by i.p. injection of Ketamine/Xylazine (80/10 mg/kg) (MilliporeSigma, St Louis, MO, USA), and ophthalmic ointment was applied to eyes. The scalp was shaved and was sterilized with 70% EtOH. For cranial window formation, a ~3×3 mm round area of right parietal skull was carefully removed. Using dental cement (Lang Dental Manufacturing, Wheeling, IL, USA), a crown was made around the cranial window, and the brain was covered with PBS. Texas-Red conjugated 2k Dalton dextran (Nanocs) was injected into the tail vein (100 μl of 1 mg/ml in saline) to visualize blood vessels in dura mater. Anesthetized mice were imaged with a single photon confocal microscope (Carl Zeiss) using a 40X water immersion with 1.0 NA objective. The vessel diameter was measured using ImageJ software.

Immunofluorescence imaging in dura mater—Animals were anesthetized with Ketamine/Xylazine (80/10 mg/kg) (MilliporeSigma, St Louis, MO, USA) before cardiac perfusion fixation in 4% paraformaldehyde. After fixation, the dura mater was dissected and postfixed for 24 hours in 4% paraformaldehyde. The collected tissues were incubated with primary antibodies: CRF (Santa Cruz), βIII-tubulin (Abcam), and Rhodamine Avidin D (Vector laboratories) for 24 hours. Tissues were then incubated with the fluorescent-dye labeled polyclonal secondary antibodies; Alexa-Fluor 488 or 647 (1:500; Invitrogen), and slides were cover-slipped using mounting medium (Invitrogen). Degranulated mast cells were determined by direct observation of scattered granules adjacent to the cell.

Mast cell imaging—For Ca^{2+} imaging, the cell suspensions were seeded onto glass coverslips as above at a density of 5,000 cells/ml, and incubated for 2 hours (37°C, 5% CO_2). The cells were loaded with Fluo-8 Ca^{2+} dye (5 μM) for 30 minutes and then imaged in Ca^{2+} imaging buffer (CIB; 125 mM NaCl, 3 mM KCl, 2.5 mM $CaCl_2$, 0.6 mM $MgCl_2$, 10 mM HEPES, 20 mM glucose, 1.2 mM $NaHCO_3$, 20 mM sucrose, adjusted to pH 7.4 with NaOH) using a confocal (Carl Zeiss, Oberkochen, Germany) or widefield fluorescence microscope (Carl Zeiss) system.

Ca^{2+} imaging in HEK293 Cells—HEK293 cells were cultured in DMEM-FBS media and maintained in a 5% CO_2 incubator at 37°C. Prior to transfection, cells were trypsinized and plated onto poly-D-lysine-coated coverslip in 35 mm culture dishes. Following overnight incubation, the cells were transiently transfected with lipofectamine 2000 (Invitrogen), using a total of 2 μg cDNA per dish (35 mm). Plasmid DNAs encoding the human MrgprX2 (pcDNA3.1) and mouse MrgprB2 (pcDNA3.1), provided by Professor

Dr. Xinzhong Dong (Johns Hopkins University, MD, USA), were co-transfected with Gα15 (pcDNA3.1) at a ratio of 9:1. A surrogate expression marker, tdTomato (60 ng), was co-transfected along with other plasmids. Forty-eight hours following transfection, cells were loaded with AM esters of the Ca^{2+} indicator Fluo-8 (1 μM; Abcam, Cambridge, MA, USA) along with Pluronic F-127 (0.04%; Life Technologies, Carlsbad, CA, USA) for 30–45 min at 37°C in the dark, in standard extracellular solution (SES) containing 140 mM NaCl, 4 mM KCl, 2 mM $CaCl_2$, 1 mM $MgCl_2$, 10 mM HEPES, 10 mM D-glucose, pH 7.40. Cells were viewed on an upright Zeiss Examiner/A1 microscope fitted with a 40× water-immersion objective (0.75-NA, 2.1-mm free working distance, Carl Zeiss) and imaged with an Axiocam 705 color camera (Carl Zeiss). Fluorescence images were taken every 5 s interval using the Zeiss Zen Blue software module. Cells were imaged in SES at room temperature; drugs were bath applied into the chamber following 10 cycles of baseline imaging, and responses were monitored for an additional 50 cycles. The percentage of cells responding to the CRF among total tdTomato-expressing cells was calculated to quantify the CRF response.

Western blot for CRF of dura mater—Tissue lysates were prepared and were analyzed by western blot as previously described[60,61]. Briefly, the collected dura mater was homogenized and centrifuged for 30 min at 12,000 rpm. Tissue lysates from 3 animals were pooled because of low protein concentration. The protein samples were separated by SDS-PAGE and then transferred to a PVDF membrane (Amersham, Buckinghamshire, UK), which was immunoblotted with anti-CRF (Santa Cruz, 1:500) and anti-β-actin (Cell Signaling, 1:5000)[62]. Protein expression was quantitated using ImageJ (NIH) and was normalized to β-actin in the same sample.

ELISA—Dura mater and blood were collected between 8:00 to 10:00 a.m. after alcohol withdrawal. Blood was collected in vacutainers containing K_3EDTA and was centrifugation at 1000 rcf for 15 min at 4°C. CRF and TNF-α levels were determined using CRH ELISA kit and TNF alpha ELISA kit (antibodies-online Inc, Limerick, PA, USA).

Mast cell degranulation assay—Mast cell degranulation was measured using β-hexosaminidase release as previously described[63]. Isolated mouse mast cells were cultivated for one week and then were sensitized overnight with mouse monoclonal anti-DNP-IgE (MilliporeSigma). Cells were washed three times and then resuspended in HEPES buffer. The cells were incubated with CRF (Phoenix Pharmaceuticals) and Compound 48/80 (MilliporeSigma) for 45 minutes at 37°C. The β-hexosaminidase released into the supernatants and cell lysates was quantified by hydrolysis of p-nitrophenyl N-acetyl-β-D-glucosamine (MilliporeSigma) in 0.1 M sodium citrate buffer (pH 4.5) for 90 minutes at 37°C. The percentage of β-hexosaminidase release was calculated as a percent of total β-hexosaminidase content.

QUANTIFICATION AND STATISTICAL ANALYSIS

Group data were expressed as mean ± S.E.M. Two-tailed unpaired Student’s t test, one-way ANOVA tests, and two-way ANOVA tests were used to determine significance in statistical comparisons, and differences were considered significant at $p < 0.05$.

Supplementary Material

Refer to Web version on PubMed Central for supplementary material.

ACKNOWLEDGEMENTS

We thank Gregory Dussor and members of the Gregory Dussor laboratory for advice on the facial von Frey test and dura injection. This work was supported by National Institutes of Health grants (NIH/NIDCR, DE026677, DE031477 to Y.S.K.), University of Texas Health Science Center at San Antonio (UTHSA) startup fund (Y.S.K.), and a Rising STAR Award (Y.S.K.) from University of Texas System.

REFERENCES

1. Gonçalves PD, Moura HF, do Amaral RA, Castaldelli-Maia JM, and Malbergier A (2020). Alcohol Use and COVID-19: Can we Predict the Impact of the Pandemic on Alcohol Use Based on the Previous Crises in the 21st Century? A Brief Review. Front. Psychiatry 11, 1–10. 10.3389/fpsyt.2020.581113. [PubMed: 32116830]
2. Egli M, Koob GF, and Edwards S (2012). Alcohol dependence as a chronic pain disorder. Neurosci. Biobehav. Rev 36, 2179–2192. 10.1016/j.neubiorev.2012.07.010. [PubMed: 22975446]
3. García-Azorín D, Aparicio-Cordero L, Talavera B, Johnson A, Schytz HW, and Guerrero-Peral ÁL (2020). Clinical characterization of delayed alcohol-induced headache. Neurology 95, e2161–e2169. 10.1212/wnl.0000000000010607. [PubMed: 32873689]
4. Zale EL, Maisto SA, and Ditre JW (2015). Interrelations between pain and alcohol: An integrative review. Clin. Psychol. Rev 37, 57–71. 10.1016/j.cpr.2015.02.005. [PubMed: 25766100]
5. Koob GF (2021). Drug Addiction: Hyperkatifeia/Negative Reinforcement as a Framework for Medications Development. Pharmacol. Rev 73, 163–201. 10.1124/pharmrev.120.000083. [PubMed: 33318153]
6. Yu W, Hwa LS, Makhijani VH, Besheer J, and Kash TL (2019). Chronic inflammatory pain drives alcohol drinking in a sex-dependent manner for C57BL/6J mice. Alcohol 77, 135–145. 10.1016/j.alcohol.2018.10.002. [PubMed: 30300665]
7. Brennan KC, and Pietrobon D (2018). A Systems Neuroscience Approach to Migraine. Neuron 97, 1004–1021. 10.1016/j.neuron.2018.01.029. [PubMed: 29518355]
8. Iyengar S, Johnson KW, Ossipov MH, and Aurora SK (2019). CGRP and the Trigeminal System in Migraine. Headache 59, 659–681. 10.1111/head.13529. [PubMed: 30982963]
9. Ashina M, Hansen JM, Á Dunga BO, and Olesen J (2017). Human models of migraine-short-Term pain for long-Term gain. Nat. Rev. Neurol 13, 713–724. 10.1038/nrneurol.2017.137. [PubMed: 28984313]
10. Strassman AM, Raymond SA, and Burstein R (1996). Sensitization of meningeal sensory neurons and the origin of headaches. Nature 384, 560–564. 10.1038/384560a0. [PubMed: 8955268]
11. Koyuncu Irmak D, Kilinc E, and Tore F (2019). Shared fate of meningeal mast cells and sensory neurons in migraine. Front. Cell. Neurosci 13, 1–10. 10.3389/fncel.2019.00136. [PubMed: 30723396]
12. Levy D (2009). Migraine pain, meningeal inflammation, and mast cells. Curr. Pain Headache Rep 13, 237–240. 10.1007/s11916-009-0040-y. [PubMed: 19457286]
13. Bienenstock J, MacQueen G, Sestini P, Marshall JS, Stead RH, and Perdue MH (1991). Mast cell/nerve interactions in vitro and in vivo. Am. Rev. Respir. Dis 143, S55–8. 10.1164/ajrccm/143.3_Pt_2.S55. [PubMed: 2003692]
14. Gaudenzio N, Sibilano R, Marichal T, Starkl P, Reber LL, Cenac N, McNeil BD, Dong X, Hernandez JD, Sagi-Eisenberg R, et al. (2016). Different activation signals induce distinct mast cell degranulation strategies. J. Clin. Invest 126, 3981–3998. 10.1172/JCI85538. [PubMed: 27643442]
15. McNeil BD, Pundir P, Meeker S, Han L, Undem BJ, Kulka M, and Dong X (2015). Identification of a mast-cell-specific receptor crucial for pseudo-allergic drug reactions. Nature 519, 237–241. 10.1038/nature14022. [PubMed: 25517090]

16. Green DP, Limjunyawong N, Gour N, Pundir P, and Dong X (2019). A Mast-Cell-Specific Receptor Mediates Neurogenic Inflammation and Pain. Neuron 101, 412–420.e3. 10.1016/j.neuron.2019.01.012. [PubMed: 30686732]

17. Navratilova E, and Porreca F (2019). Substance P and Inflammatory Pain: Getting It Wrong and Right Simultaneously. Neuron 101, 353–355. 10.1016/j.neuron.2019.01.034. [PubMed: 30731054]

18. Basbaum AI, Bautista DM, Scherrer G, and Julius D (2009). Cellular and Molecular Mechanisms of Pain. Cell 139, 267–284. 10.1016/j.cell.2009.09.028. [PubMed: 19837031]

19. Charity Fix BL (2015). A Role for Mast Cells in Alcohol-Induced Tissue Damage and Remodeling. J. Clin. Exp. Pathol 05. 10.4172/2161-0681.1000218.

20. Wimberly AL, Forsyth CB, Khan MW, Pemberton A, Khazaie K, and Keshavarzian A (2013). Ethanol-Induced Mast Cell-Mediated Inflammation Leads to Increased Susceptibility of Intestinal Tumorigenesis in the APCΔ468 Min Mouse Model of Colon Cancer. Alcohol. Clin. Exp. Res 37, 199–208. 10.1111/j.1530-0277.2012.01894.x.

21. Mendes LO, Amorim JPA, Teixeira GR, Chuffa LGA, Fioruci BA, Pimentel TA, de Mello W, Padovani CR, Pereira S, Martinez M, et al. (2011). Mast cells and ethanol consumption: Interactions in the prostate, epididymis and testis of UChB rats. Am. J. Reprod. Immunol 66, 170–178. 10.1111/j.1600-0897.2010.00958.x. [PubMed: 21241399]

22. Romero-Reyes M, and Akerman S (2014). Update on Animal Models of Migraine. Curr. Pain Headache Rep 18. 10.1007/s11916-014-0462-z.

23. Gianoulakis C, Dai X, and Brown T (2003). Effect of chronic alcohol consumption on the activity of the hypothalamic-pituitary-adrenal axis and pituitary β-endorphin as a function of alcohol intake, age, and gender. Alcohol. Clin. Exp. Res 27, 410–423. 10.1097/01.ALC.0000056614.96137.B8. [PubMed: 12658106]

24. Inder WJ, Joyce PR, Ellis MJ, Evans MJ, Livesey JH, and Donald RA (1995). The effects of alcoholism on the hypothalamic-pituitary adrenal axis: Interaction with endogenous opioid peptides. Clin. Endocrinol. (Oxf) 43, 283–290. 10.1111/j.1365-2265.1995.tb02033.x. [PubMed: 7586596]

25. Waltman C, Blevins LS, Boyd G, and Wand GS (1993). The effects of mild ethanol intoxication on the hypothalamic-pituitary-adrenal axis in nonalcoholic men. J. Clin. Endocrinol. Metab 77, 518–522. 10.1210/jcem.77.2.8393888. [PubMed: 8393888]

26. Li X, and Bartlett WP (1991). Developmental expression of glial fibrillary acidic protein and glutamine synthetase mRNAs in normal and jimpy mice. Mol. Brain Res 9, 313–317. [PubMed: 1674813]

27. Economidou D, Cippitelli A, Stopponi S, Braconi S, Clementi S, Ubaldi M, Martin-Fardon R, Weiss F, Massi M, and Ciccocioppo R (2011). Activation of Brain NOP Receptors Attenuates Acute and Protracted Alcohol Withdrawal Symptoms in the Rat. Alcohol. Clin. Exp. Res 35, 747–755. 10.1111/j.1530-0277.2010.01392.x. [PubMed: 21223310]

28. Kempuraj D, Mentor S, Thangavel R, Ahmed ME, Selvakumar GP, Raikwar SP, Dubova I, Zaheer S, Iyer SS, and Zaheer A (2019). Mast cells in stress, pain, blood-brain barrier, neuroinflammation and alzheimer's disease. Front. Cell. Neurosci 13, 1–11. 10.3389/fncel.2019.00054. [PubMed: 30723396]

29. Theoharides TC, Donelan J, Kandere-Grzybowska K, and Konstantinidou A (2005). The role of mast cells in migraine pathophysiology. Brain Res. Rev 49, 65–76. 10.1016/j.brainresrev.2004.11.006. [PubMed: 15960987]

30. Theoharides TC, K. Singh L, Boucher W, Pang X, Letourneau R, Webster E, and Chrousos G (1998). Corticotropin-releasing hormone induces skin mast cell degranulation and increased vascular permeability, a possible explanation for its proinflammatory effects. Endocrinology 139, 403–413. 10.1210/endo.139.1.5660. [PubMed: 9421440]

31. Burgos-Vega CC, Quigley LD, Trevisan dos Santos G, Yan F, Asiedu M, Jacobs B, Motina M, Safdar N, Yousuf H, Avona A, et al. (2019). Non-invasive dural stimulation in mice: A novel preclinical model of migraine. Cephalalgia 39, 123–134. 10.1177/0333102418779557. [PubMed: 29848109]

32. Avona A, Burgos-Ega C, Burton MD, Akopian AN, Price TJ, and Dussor G (2019). Dural calcitonin gene-related peptide produces female-specific responses in rodent migraine models. J. Neurosci 39, 4323–4331. 10.1523/JNEUROSCI.0364-19.2019. [PubMed: 30962278]
33. Theoharides TC, Tsilioni I, and Ren H (2019). Recent advances in our understanding of mast cell activation - or should it be mast cell mediator disorders? Expert Rev. Clin. Immunol 15, 639–656. 10.1080/1744666X.2019.1596800. [PubMed: 30884251]
34. D'Costa S, Ayyadurai S, Gibson AJ, Mackey E, Rajput M, Sommerville LJ, Wilson N, Li Y, Kubat E, Kumar A, et al. (2019). Mast cell corticotropin-releasing factor subtype 2 suppresses mast cell degranulation and limits the severity of anaphylaxis and stress-induced intestinal permeability. J. Allergy Clin. Immunol 143, 1865–1877.e4. 10.1016/j.jaci.2018.08.053. [PubMed: 30439403]
35. Mason BN, and Russo AF (2018). Vascular contributions to migraine: Time to revisit? Front. Cell. Neurosci 12, 1–10. 10.3389/fncel.2018.00233. [PubMed: 29386999]
36. Burstein R, Yarnitsky D, Goor-Aryeh I, Ransil BJ, and Bajwa ZH (2000). An association between migraine and cutaneous allodynia. Ann. Neurol 47, 614–624. 10.1002/1531-8249(200005)47:5<614::AID-ANA9>3.0.CO;2-N. [PubMed: 10805332]
37. Smith ML, Walcott AT, Heinricher MM, and Ryabinin AE (2017). Anterior cingulate cortex contributes to alcohol withdrawal- induced and socially transferred hyperalgesia. eNeuro 4, 1–10. 10.1523/ENEURO.0087-17.2017.
38. De Logu F, Puma SL, Landini L, Portelli F, Innocenti A, De Araujo DSM, Janal MN, Patacchini R, Bunnett NW, Geppetti P, et al. (2019). Schwann cells expressing nociceptive channel TRPA1 orchestrate ethanol-evoked neuropathic pain in mice. J. Clin. Invest 129, 5424–5441. 10.1172/JCI128022. [PubMed: 31487269]
39. Dina OA, Barletta J, Chen X, Mutero A, Martin A, Messing RO, and Levine JD (2000). Key Role for the Epsilon Isoform of Protein Kinase C in Painful Alcoholic Neuropathy in the Rat. 20, 8614–8619.
40. Orellana JA, Cerpa W, Carvajal MF, Lerma-Cabrera JM, Karahanian E, Osorio-Fuentealba C, and Quintanilla RA (2017). New Implications for the Melanocortin System in Alcohol Drinking Behavior in Adolescents: The Glial Dysfunction Hypothesis. Front. Cell. Neurosci 11, 90. 10.3389/fncel.2017.00090. [PubMed: 28424592]
41. Rozas P, Lazcano P, Piña R, Cho A, Terse A, Pertusa M, Madrid R, Gonzalez-Billault C, Kulkarni AB, and Utreras E (2016). Targeted overexpression of tumor necrosis factor-α increases cyclin-dependent kinase 5 activity and TRPV1-dependent Ca2+ influx in trigeminal neurons. Pain 157, 1346–1362. 10.1097/j.pain.0000000000000527. [PubMed: 26894912]
42. Mostofsky E, Bertisch SM, Vgontzas A, Buettner C, Li W, Rueschman M, and Mittleman MA (2020). Prospective cohort study of daily alcoholic beverage intake as a potential trigger of headaches among adults with episodic migraine. Ann. Med 52, 386–392. 10.1080/07853890.2020.1758340. [PubMed: 32306754]
43. Panconesi A (2016). Alcohol-induced headaches: Evidence for a central mechanism? J. Neurosci. Rural Pract 7, 269–275. 10.4103/0976-3147.178654. [PubMed: 27114660]
44. Wiese JG, Shlipak MG, and Browner WS (2000). The alcohol hangover. Ann. Intern. Med 132, 897–902. 10.7326/0003-4819-132-11-200006060-00008. [PubMed: 10836917]
45. Sjaastad O, and Bakketeig LS (2004). Hangover headache: Accompanying symptoms. Vågå study of headache epidemiology. J. Headache Pain 5, 224–229. 10.1007/s10194-004-0130-5.
46. Levy D, Burstein R, Kainz V, Jakubowski M, and Strassman AM (2007). Mast cell degranulation activates a pain pathway underlying migraine headache. Pain 130, 166–176. 10.1016/j.pain.2007.03.012. [PubMed: 17459586]
47. Cao J, Papadopoulou N, Kempuraj D, Boucher WS, Sugimoto K, Cetrulo CL, and Theoharides TC (2005). Human Mast Cells Express Corticotropin-Releasing Hormone (CRH) Receptors and CRH Leads to Selective Secretion of Vascular Endothelial Growth Factor. J. Immunol 174, 7665–7675. 10.4049/jimmunol.174.12.7665. [PubMed: 15944267]
48. Asadi S, Alysandratos KD, Angelidou A, Miniati A, Sismanopoulos N, Vasiadi M, Zhang B, Kalogeromitros D, and Theoharides TC (2012). Substance P (SP) induces expression of functional corticotropin-releasing hormone receptor-1 (CRHR-1) in human mast cells. J. Invest. Dermatol 132, 324–329. 10.1038/jid.2011.334. [PubMed: 22089831]

49. Zhang X, Wang Y, Dong H, Xu Y, and Zhang S (2016). Induction of microglial activation by mediators released from mast cells. Cell. Physiol. Biochem 38, 1520–1531. 10.1159/000443093. [PubMed: 27050634]
50. Gupta K, and Harvima IT (2018). Mast cell-neural interactions contribute to pain and itch. Immunol. Rev 282, 168–187. 10.1111/imr.12622. [PubMed: 29431216]
51. Tatemoto K, Nozaki Y, Tsuda R, Konno S, Tomura K, Furuno M, Ogasawara H, Edamura K, Takagi H, Iwamura H, et al. (2006). Immunoglobulin E-independent activation of mast cell is mediated by Mrg receptors. Biochem. Biophys. Res. Commun 349, 1322–1328. 10.1016/j.bbrc.2006.08.177. [PubMed: 16979137]
52. Chartoff EH, and Carlezon WA (2014). Drug withdrawal conceptualized as a stressor. Behav. Pharmacol 25, 473–492. 10.1097/FBP.0000000000000080. [PubMed: 25083570]
53. Kim YS, Anderson M, Park K, Zheng Q, Agarwal A, Gong C, Saijilafu, Young LA, He S, LaVinka PC, et al. (2016). Coupled Activation of Primary Sensory Neurons Contributes to Chronic Pain. Neuron 91, 1085–1096. 10.1016/j.neuron.2016.07.044. [PubMed: 27568517]
54. Kim YS, Chu Y, Han L, Li M, Li Z, LaVinka PC, Sun S, Tang Z, Park K, Caterina MJ, et al. (2014). Central terminal sensitization of TRPV1 by descending serotonergic facilitation modulates chronic pain. Neuron 81, 873–887. 10.1016/j.neuron.2013.12.011. [PubMed: 24462040]
55. Chaplan SR, Bach FW, Pogrel JW, Chung JM, and Yaksh TL (1994). Quantitative assessment of tactile allodynia in the rat paw. J. Neurosci. Methods 53, 55–63. 10.1016/0165-0270(94)90144-9. [PubMed: 7990513]
56. Langford DJ, Bailey AL, Chanda ML, Clarke SE, Drummond TE, Echols S, Glick S, Ingrao J, Klassen-Ross T, Lacroix-Fralish ML, et al. (2010). Coding of facial expressions of pain in the laboratory mouse. Nat. Methods 7, 447–449. 10.1038/nmeth.1455. [PubMed: 20453868]
57. Gulyás M, Bencsik N, Pusztai S, Liliom H, and Schlett K (2016). AnimalTracker: An ImageJ-Based Tracking API to Create a Customized Behaviour Analyser Program. Neuroinformatics 14, 479–481. 10.1007/s12021-016-9303-z. [PubMed: 27166960]
58. Elshamy WM, and Ernfors P (1996). Requirement of neurotrophin-3 for the survival of proliferating trigeminal ganglion progenitor cells. Development 122, 2405–2414. [PubMed: 8756286]
59. Lagares A, Li HY, Zhou XF, and Avendaño C (2007). Primary sensory neuron addition in the adult rat trigeminal ganglion: Evidence for neural crest glio-neuronal precursor maturation. J. Neurosci 27, 7939–7953. 10.1523/JNEUROSCI.1203-07.2007. [PubMed: 17652585]
60. Wierzbicka JM, Żmijewski MA, Piotrowska A, Nedoszytko B, Lange M, Tuckey RC, and Slominski AT (2016). Bioactive forms of vitamin D selectively stimulate the skin analog of the hypothalamus-pituitary-adrenal axis in human epidermal keratinocytes. Mol. Cell. Endocrinol 437, 312–322. 10.1016/j.mce.2016.08.006. [PubMed: 27524410]
61. Cabeza L, Ramadan B, Giustiniani J, Houdayer C, Pellequer Y, Gabriel D, Fauconnet S, Haffen E, Risold PY, Fellmann D, et al. (2021). Chronic exposure to glucocorticoids induces suboptimal decision-making in mice. Eur. Neuropsychopharmacol 10.1016/j.euroneuro.2021.01.094.
62. Upadhaya R, Mizunoya W, and Anderson JE (2011). Detecting multiple proteins by Western blotting using same-species primary antibodies, precomplexed serum, and hydrogen peroxide. Anal. Biochem 419, 342–344. 10.1016/j.ab.2011.08.014. [PubMed: 21888891]
63. Kuehn HS, Radinger M, and Gilfillan AM (2010). Measuring mast cell mediator release. Curr. Protoc. Immunol Chapter 7, Unit 7.38. 10.1002/0471142735.im0738s91.

Highlights

- Alcohol withdrawal causes headache behaviors, depending on the presence of MrgprB2
- Alcohol withdrawal-induced sensitization of TG is absent in MrgprB2-lacking mice
- Mast cell degranulation by MrgprB2 in dura mater induces alcohol withdrawal headache
- MrgprB2 receptor mediates the development of alcohol withdrawal-associated headache

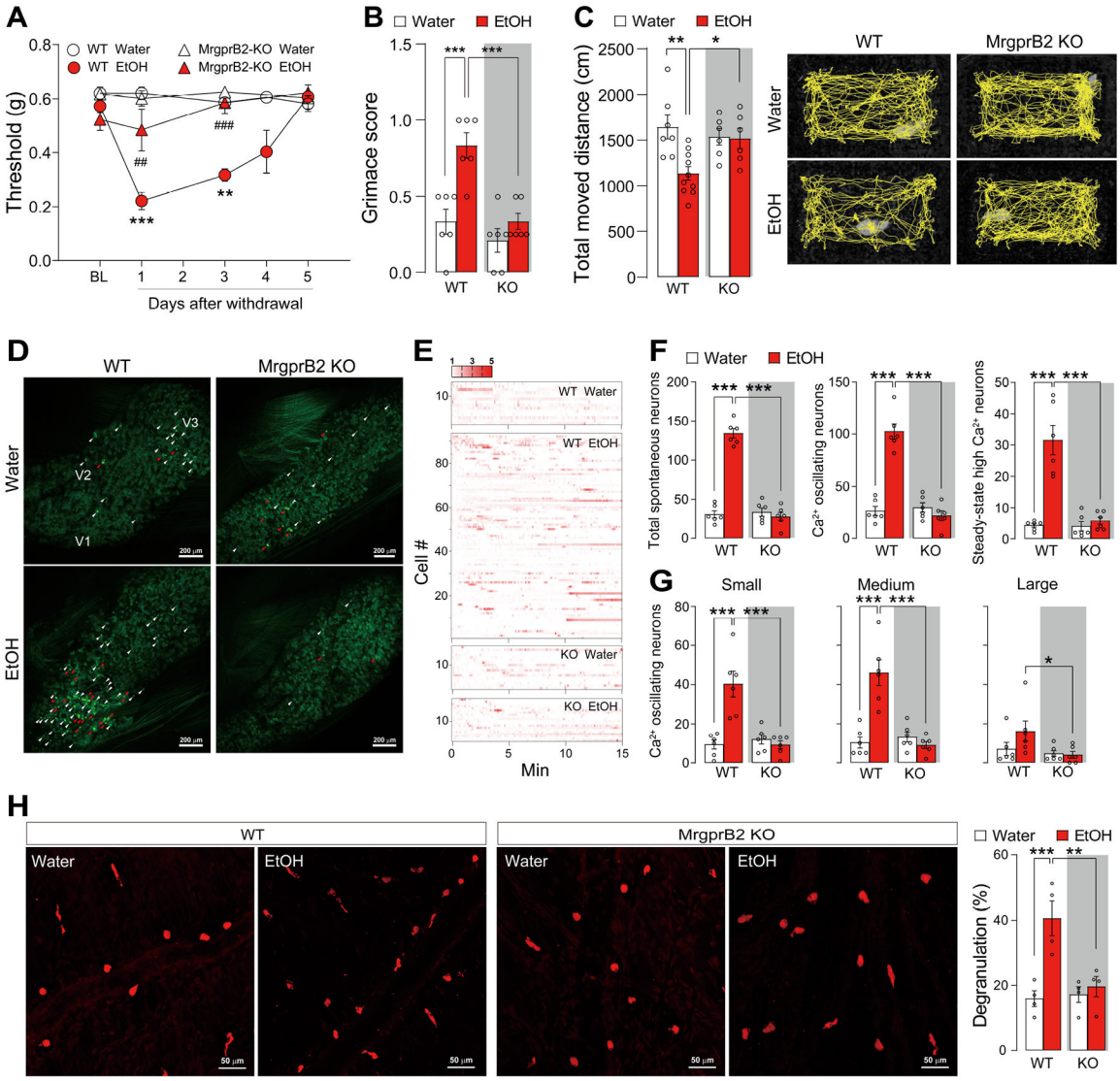

Figure 1. MrgprB2-Induced Mast Cell Degranulation Contributes to Alcohol Withdrawal-Induced Headache and Pain Behaviors and Sensitization of TG Neurons

(A) Facial mechanical withdrawal thresholds at various time points after alcohol withdrawal following 3 weeks of voluntary ethanol consumption vs. water only control in wild type (WT) or MrgprB2-deficient (KO) mice (n = 6 mice).

(B) Grimace score measured 24 hours after alcohol withdrawal (n = 6 mice).

(C) (*left*) Total distance moved in 5 min open field test performed 24 hours after alcohol withdrawal. (*right*) Representative traces of total distance moved in 5 mins (n = 6–10 mice).

(D) Representative Pirt-GCaMP3 Ca^{2+} imaging of spontaneous activity in *in vivo* intact TG after alcohol withdrawal. V1 (ophthalmic), V2 (maxillary), and V3 (mandibular) indicate location of neuronal cell bodies in TG image. Neurons exhibiting spontaneous Ca^{2+} oscillation (white arrowheads). Neurons exhibiting spontaneous steady-state high Ca^{2+} activity (red arrowheads).

(E) Representative heatmaps of spontaneously activated individual neurons.

(F) Number of total oscillating and steady-state high Ca^{2+} spontaneously activated neurons (n = 6 mice).
(G) Number of Ca^{2+} oscillating neurons stratified by cell diameter. Small-diameter TG neurons (<20 μm); medium (20–25 μm); large (>25 μm) (n = 6 mice).
(H) (*left*) Representative confocal fluorescent images of mast cells in dura mater. Mast cells (red) were identified by avidin staining. (*right*) Percent degranulation of mast cells in each group (n = 4 mice).
TG: trigeminal ganglia. Quantitative data are expressed as mean±SEM. *p < 0.05; **p < 0.01; ***p < 0.001 by (A) two-way ANOVA with Bonferroni's multiple comparison post-hoc test and (B-H) one-way ANOVA with Dunnett's multiple comparison post-hoc test.

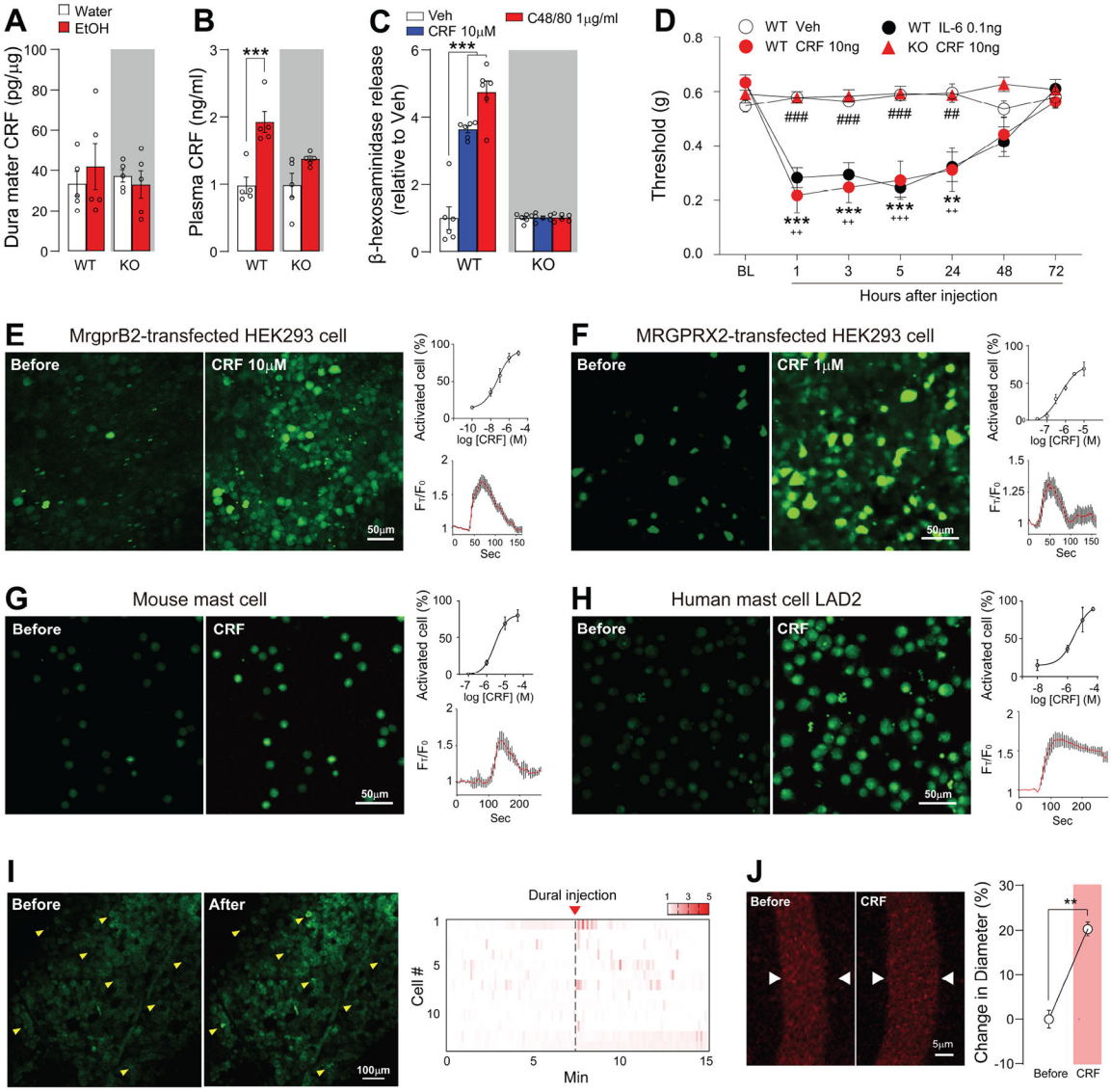

Figure 2. CRF-Mediated Mast Cell Activation via MrgprB2 Induces Headache Behaviors

(A and B) CRF levels in dura mater (A) and plasma (B) (n = 5 mice).

(C) β-hexosaminidase release by mouse peritoneal mast cells (n = 6 wells)

(D) Facial mechanical withdrawal thresholds after dural injection with IL-6 (0.1 ng) or CRF (10 ng) in wild type (WT) or MrgprB2-deficient (KO) mice (n = 6–8 mice). *WT Veh. vs. WT CRF; $^{+}$WT Veh. vs. WT IL-6; $^{\#}$WT CRF vs. KO CRF.

(E and F) Representative Fluo-8 Ca^{2+} dye fluorescent images showing $[Ca^{2+}]_{in}$ increase in HEK293 cells expressing MrgprB2 (E) or MrgprX2 (F) before and after bath application of CRF (10 μM or 1 μM CRF). (*right, top*) Percentage of total cells activated by CRF bath application in MrgprB2-transfected (n = 11 cultures) (E) or MrgprX2-transfected HEK293 cells (n = 14 cultures) (F). (*right, bottom*) Average Ca^{2+} transient trace of cells activated by CRF from MrgprB2 (10 μM CRF)-transfected (E) or MrgprX2 (1 μM CRF)-transfected (F) HEK293 cells.

(G and H) (*left*) Representative Fluo-8 Ca^{2+} dye fluorescent images showing $[Ca^{2+}]_{in}$ increase by CRF (50 μM) bath application in isolated mouse mast cells (G) or LAD2 human mast cells (H). (*right, top*) Percentage of total cells activated by CRF bath application from isolated mouse mast cells (n = 12 cultures) (G) or LAD2 human mast cells (n = 11 cultures) (H). (*right, bottom*) Average Ca^{2+} transient trace of cells activated by CRF (50 μM) from isolated mouse mast cells (G) or LAD2 human mast cells (H).

(I) (*left*) Representative TG images of spontaneous neuronal activities before (*left image*) and after (*right image*) direct CRF dural injection using *in vivo* intact TG Pirt-GcaMP3 Ca^{2+} imaging. (*right*) Heatmap showing $[Ca^{2+}]_{in}$ increase in TG neurons after direct CRF dural injection. This experiment was performed three times. Yellow arrowheads indicate TG neurons. After CRF (10 ng) injection activated neurons in dura are visible.

(J) (*left*) Representative *in vivo* fluorescent images of dura blood vessel (red) stained with Texas red dye (tail vein injection). (*right*) Percentage change in blood vessel diameter after CRF (20 μM) application in dura mater through cranial window (n = 3 mice). Dura blood vessel images were captured by confocal microscopy.

CRF: corticotropin-releasing factor, IL6: interleukin-6, TG: trigeminal ganglia. Quantitative data are expressed as mean±SEM. *$p < 0.05$; **$p < 0.01$; ***$p < 0.001$ by (J) two-tailed unpaired Student's t test, (B and C) one-way ANOVA with Dunnett's multiple comparison post-hoc test, and (D) two-way ANOVA with Tukey's multiple comparison post-hoc test.

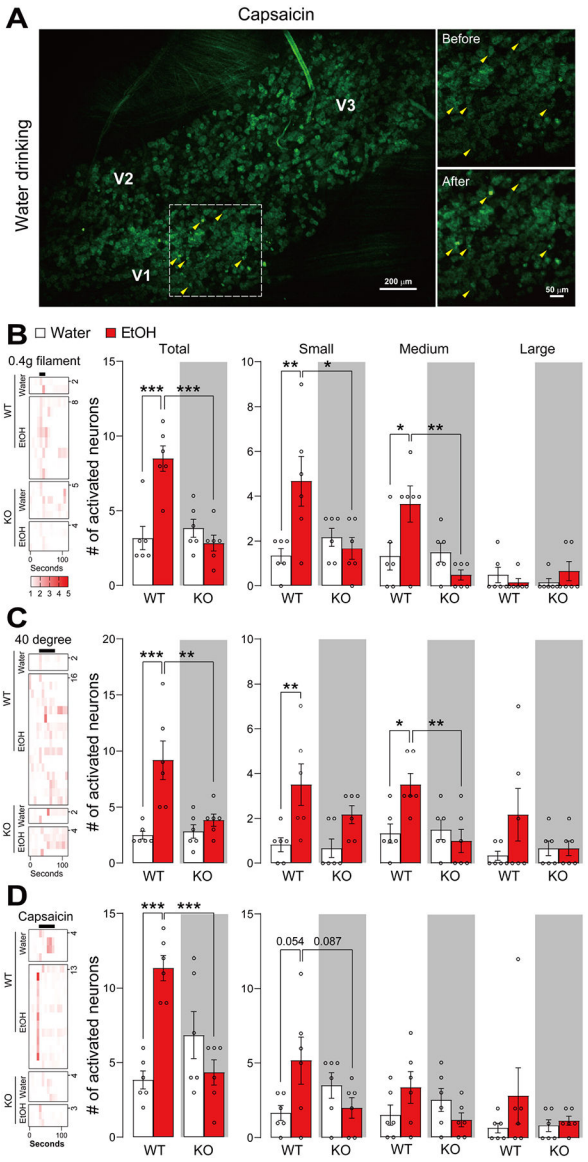

Figure 3. MrgprB2 Deletion Prevents Sensitization (mechanical, thermal, and chemical) of TG Neurons after Alcohol Withdrawal

(A) Representative images of *in vivo* TG neurons activated by direct capsaicin (500 μM, 10 μL) injection into V1 region in water-fed control mice. Capsaicin was subcutaneously injected into the V1 branch (periorbital) region using an insulin syringe; *In vivo* intact TG Pirt-GCaMP3 Ca^{2+} imaging was performed after alcohol withdrawal. V1 (ophthalmic), V2 (maxillary), and V3 (mandibular) indicate location of neuron cell bodies in TG image. Yellow arrowheads indicate TG neurons in V1 region. Activated neurons are visible after, but not before, capsaicin injection into V1 region.

(B-D) Heatmaps and number of individual TG neurons activated by 0.4 g von Frey filament (B), mild hot water (40°C) (C), or capsaicin (D) (n = 6 mice). Number of activated neurons in response to various stimuli was plotted according to the size (small, medium, large) of each member of the pair. Small-diameter TG neurons (<20 μm); medium (20–25 μm); large (>25 μm).

TG: trigeminal ganglia. Quantitative data are expressed as mean±SEM. *p < 0.05; **p < 0.01; ***p < 0.001, one-way ANOVA with Dunnett's multiple comparison post-hoc test.

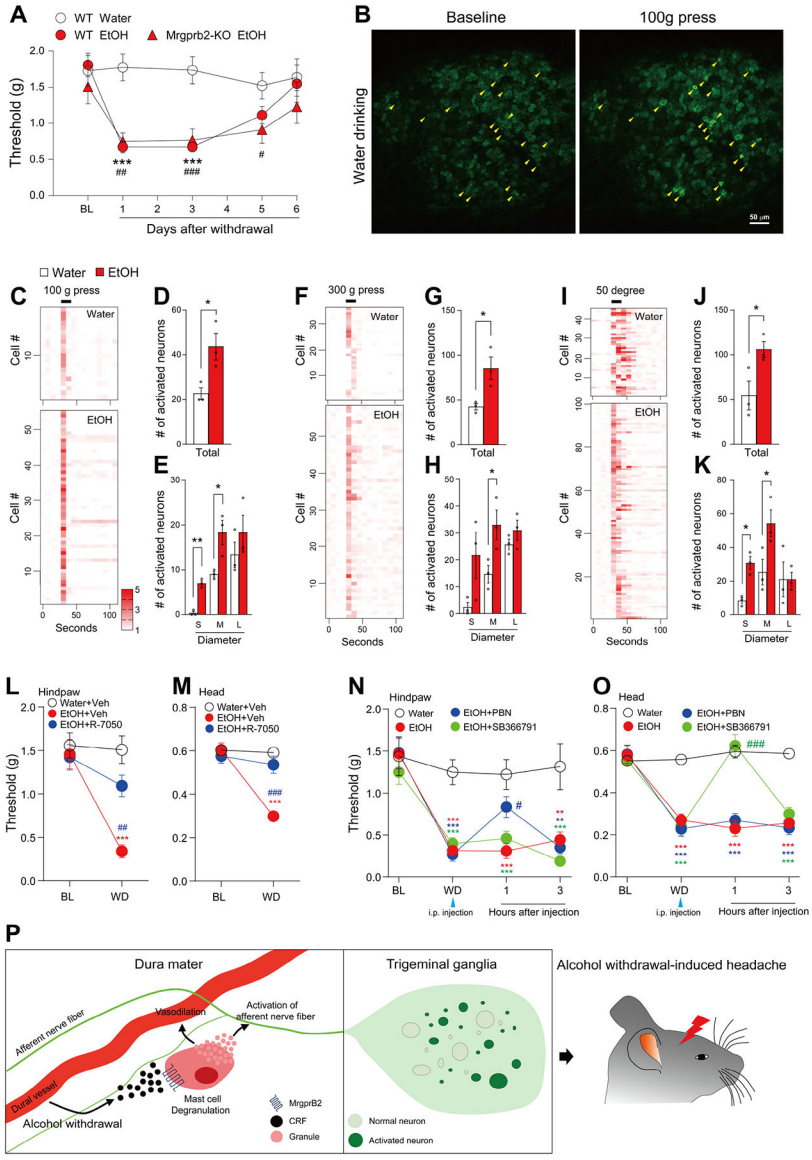

Figure 4. Head Hypersensitivity and Hindpaw Hypersensitivity Driven by Alcohol Withdrawal Involve Distinctive Mechanisms

(A) Hindpaw mechanical withdrawal thresholds at various time points after alcohol withdrawal following 3 weeks of voluntary ethanol consumption vs. water only control in wild type (WT) or MrgprB2-deficient (KO) mice (n = 7–9 mice).

(B) Representative images of *in vivo* intact DRG Pirt-GCaMP3 Ca^{2+} imaging activated by 100 g hindpaw press in water-only control mice. Yellow arrowheads indicate DRG neurons activated by 100g hindpaw press.

(C-K) Heatmaps and numbers of individual neurons activated by 100 g press (C-E), 300 g press (F-H), or hot water (50°C, I-K) stimuli onto hindpaw (n = 3 mice). S, Small-diameter DRG neurons (<20 μm); M, medium (20–25 μm); L, large (>25 μm).

(L and M) Hindpaw mechanical (L) and head withdrawal (M) thresholds tested by von Frey filament at baseline (BL) and 24 hours after alcohol withdrawal (WD) together with

R-7050 (12 mg/kg) i.p. injection for 11 consecutive days (n = 6 mice). *(red) Water+Veh. vs. EtOH+Veh.; *(blue) EtOH +Veh. vs. EtOH+R-7050; #(blue) EtOH+Veh. vs. EtOH+R-7050. **(N and O)** Hindpaw mechanical (N) and head withdrawal (O) thresholds at 24 hours after alcohol withdrawal together with PBN (100 mg/kg) or SB366791 (1 mg/kg) i.p. injection (n = 6 mice). *(red) Water+Veh. vs. EtOH+Veh.; *(blue) Water+Veh vs. EtOH+PBN; *(green) Water+Veh. vs. EtOH+SB366791; #(blue) EtOH +Veh. vs. EtOH+PBN; #(green) EtOH +Veh. vs. EtOH+SB366791.

(P) Schematic model of alcohol withdrawal-induced headache. Alcohol withdrawal-induced CRF release from blood vessels induces mast cell degranulation in dura mater, which results in sensitization of primary sensory TG neurons and vasodilation. This pathway ultimately induces headache behavior.

CRF: corticotropin-releasing factor, DRG: dorsal root ganglia, TNF-α receptor: tumor necrosis factor-α receptor, TRPV1: transient receptor potential channel V1, ROS: reactive oxygen species, TG: trigeminal ganglia. Quantitative data are expressed as mean±SEM. *$p < 0.05$; **$p < 0.01$; ***$p < 0.001$, (C-K) two-tailed unpaired Student's t test; (L and M) one-way ANOVA with Dunnett's multiple comparison post-hoc test; (A, N, and O) two-way ANOVA with Bonferroni's multiple comparison post-hoc test.

KEY RESOURCES TABLE

REAGENT or RESOURCE	SOURCE	IDENTIFIER
Antibodies		
Anti-CRF	Santa Cruz	Cat# sc-293187; RRID: AB_2687937
βIII-tubulin	Abcam	Cat# ab18207; RRID: AB_444319
β-actin	Cell Signaling	Cat# 4970; RRID: AB_2223172
Chemicals, peptides, and recombinant proteins		
CRF	Phoenix Pharmaceuticals	019–06
IL-6	R&D Systems	406-ML
R-7050	Tocris	5432
PBN	Cayman	15412
SB366791	Tocris	1615
Astressin	Tocris	1606
Murine SCF	Peprotech	250–03
Fibronectin	MilliporeSigma	F4759
Human SCF	Peprotech	300–07
Anti-DNP-IgE	MilliporeSigma	D8406
Compound 48/80	MilliporeSigma	C2313
p-nitrophenyl N-acetyl-β-D-glucosamine	MilliporeSigma	487052
Critical commercial assays		
CRH ELISA assay	antibodies-online Inc	ABIN5593011
TNF alpha ELISA assay	antibodies-online Inc	ABIN6574140
Experimental models: Cell lines		
Human: HEK293	ATCC	CRL-1573
Human: LAD2	McNeil et al.[15]	N/A
Experimental models: Organisms/strains		
Mouse: C57BL/6 mice	The Jackson Laboratory	N/A
Mouse: Pirt-GCaMP3 mice	Kim et al.[53]	N/A
Mouse: MrgprB2-deficient mice	The Centre for Phenogenomics	N/A
Recombinant DNA		
Human MrgprX2 (pcDNA3.1)	McNeil et al.[15]	N/A
Mouse MrgprB2 (pcDNA3.1)	McNeil et al.[15]	N/A
Software and algorithms		
Prism	GraphPad software	www.graphpad.com
FIJI/ImageJ	Fiji/NIH	www.fiji.sc